Chinese Journal of
POLYMER SCIENCE

RESEARCH ARTICLE

https://doi.org/10.1007/s10118-022-2667-7
Chinese J. Polym. Sci. **2022**, *40*, 310–320

Hypercrosslinking Polymers Fabricated from Divinyl Benzene *via* Friedel-Crafts Addition Polymerization

Zheng-Yu Duan[a], Yan-Yan Wang[a], Qi-Wei Pan[a*], Yun-Feng Xie[b*], and Zhi-Yong Chen[a*]

[a] *Shandong Provincial Key Laboratory of Fluorine Chemistry and Chemical Materials, School of Chemistry and Chemical Engineering; University of Jinan, Jinan 250022, China*
[b] *Nutrition & Health Research Institute, COFCO Corporation, Beijing Key Laboratory of Nutrition & Health and Food Safety, Beijing 102209, China*

Electronic Supplementary Information

Abstract Microporous organic polymers with high surface area are widely used in many applications. Among them, hypercrosslinked polymers have been extensively concerned because of their simple processes and low-cost reagents. However, due to most state-of-the-art strategies for HCPs based on condensation reactions, the release of small molecules such as hydrochloric acid and methanol involved in such strategies brings about new hazards to environment. Herein, we propose a method of fabrication of hypercrosslinked polymers *via* self-addition polymerization of divinyl benzene and its crosslinking with polar aromatic molecules. The hypercrosslinked polyDVB-based products are demonstrated by Friedel-Crafts addition reaction of double bonds on DVB that can connect adjacent phenyl rings of aromatic molecules to form the crosslinked networks. The HCPDVB-CB obtained in 1-chlorobutane as solvent has a high micropore content and displays high surface area up to 931 m^2/g. Following this finding, DVB is used as a novel external crosslinker for knitting polar aromatic molecules. When L-phenylalanine and bisphenol A are used as the aromatic units, the obtained HCP(Phe-DVB) and HCP(BPA-DVB) could reach surface area of 612 and 471 m^2/g, and have hydrogen uptake of 0.62 wt% and 0.58 wt% at 77 K and 1.13 bar by comparison with HCPDVB-CB having hydrogen uptake of 0.30 wt%, respectively.

Keywords Hypercrosslinked polymers; Divinyl benzene; Friedel-Crafts alkylation; Microporous organic polymers; Gas storage

Citation: Duan, Z. Y.; Wang, Y. Y.; Pan, Q. W.; Xie, Y. F.; Chen, Z. Y. Hypercrosslinking polymers fabricated from divinyl benzene *via* Friedel-Crafts addition polymerization. *Chinese J. Polym. Sci.* **2022**, *40*, 310–320.

INTRODUCTION

Microporous organic polymers (MOPs) are characterized by abundant micropores (pore size below 2 nm) and high surface area that enable them to find diverse applications in many fields, such as gas storage, drug delivery, separation, and catalysis.[1–3] Generally, MOPs are categorized into covalent organic frameworks (COFs),[4,5] conjugated microporous polymers (CMPs),[6,7] covalent triazine frameworks (CTFs),[8,9] porous aromatic frameworks (PAFs),[10,11] polymers of intrinsic microporosity (PIMs),[12] porous organic cages[13] and hypercrosslinked polymers (HCPs).[14,15] Among them, HCPs are of simple preparation processes and wide monomer sources, making them suitable for scale up fabrication.[16,17]

HCPs were introduced fifty years ago, but have burst into receiving more attention due to the demand of energy storage and environmental protection in the recent decade.[18,19] The first well-known type of HCPs, Davankov resin, was invented by Tsyurupa and Davankov through Friedel-Crafts post-crosslinking of linear polystyrene or low-crosslinked poly(styrene-*co*-divinyl benzene) precursors using dichloro-molecules as external crosslinkers in the presence of Lewis acid.[20] According to the synthetic route, HCPs mainly fall into three groups: post-crosslinking of polymeric precursors,[21,22] direct one-step self-condensation polymerization of functional monomers,[23–25] and "knitting" rigid aromatic units with external crosslinkers.[26,27]

Up to date, the most efficient reaction involved in HCPs fabrication is still based on Friedel-Crafts alkylation that has been used to introduce functional groups onto the benzene ring for over 100 years,[28–30] though a few reports have been described other hypercrosslinking strategies based on radical post-polymerization,[31] isocynate-urea reaction,[32] and imidization reaction[33] in recent years. It is probably attributed to carbon-carbon bond formation during Friedel-Crafts alkylation that must accompany directly connecting of alkyl groups onto aromatic rings, leading to the rigid frameworks needed for high surface area. From the polymerization mechanism of view, Friedel-Crafts alkylation is categorized into two types: Friedel-Crafts condensation polymerization and Friedel-Crafts addition polymerization. Most of state-of-the-art strategies for synthesis of HCPs are based on Friedel-Crafts condensa-

* Corresponding authors, E-mail: chm_panqw@ujn.edu.cn (Q.W.P.)
E-mail: xieyunfeng@cofco.com (Y.F.X.)
E-mail: chm_chenzy@ujn.edu.cn (Z.Y.C.)

Received July 31, 2021; Accepted November 18, 2021; Published online January 14, 2022

tion polymerization. This process generates a new C—C bond, and relevant hydrochloric acid when dichloro-molecules are used as crosslinkers or relevant methanol when formaldehyde dimethyl acetal is used as crosslinker.[34–36] The release of small molecules would give rise to new hazards to environment.

By contrast, Friedel-Crafts addition polymerization would be a better alternative as no byproducts are released.[31] There are only a few reports on the preparation of HCPs by Friedel-Crafts addition reaction. Ando *et al*. first described the preparation of hypercrosslinked polymers by Friedel-Crafts alkylation of the residual double bonds on poly(styrene-divinyl benzene) precursors without any external crosslinkers.[37] Zeng *et al*. incorporated ester or pyrrolidone group into the PDVB precursors, then obtained more hydrophilic HCPs after post-crosslinking of the pendant double bonds.[38,39] In a previous study, we fabricated hierarchical porous hypercrosslinked PDVB cryogels by combination of redox-initiated cryopolymerization and Friedel-Crafts postcrosslinking of pendent double bonds.[40] Additionally, Liu and co-workers reported a series of HCPs with high specific surface area using octavinylsilsesquioxane (OVS), a type of polyhedral oligomeric silsesquioxane (POSS) modified by double-bond, as crosslinker to copolymerize with various aromatic molecules by Friedel-Crafts reaction, which also proved that the strategy of using double bond to link phenyl ring was feasible.[41,42]

DVB is a type of scale up commercial product that is widely used as crosslinker in numerous chain polymerizations.[43–45] It is very desirable to explore polymerization of DVB by Friedel-Crafts reaction, as it is reasonable given that DVB has two double bonds on a benzene ring. In this work, we demonstrate a facile way to prepare HCPs by one-step Friedel-Crafts addition polymerization of DVB. In this reaction, divinylbenzene shows good self-polymerization behavior in the presence of Lewis acid, and it can also be used as an additional crosslinker to connect polar aromatic molecules, such as phenol, bisphenol A,L-phenylalanine and L-tyrosine. The synthesis method is mild, low cost and non-polluting. The surface area and porosity of the prepared HCPs can be adjusted by reaction conditions, and the resulting materials show promising characteristics for hydrogen storage.

EXPERIMENTAL

Materials

Divinylbenzene (DVB, containing 80% of 1,3- and 1,4-DVB isomers) was purchased from Aladdin Chemistry Co., Ltd. (Shanghai, China) and free from inhibitor by passing through basic Al_2O_3 (Sinopharm Chemical Reagent Co., Ltd., Shanghai, China). Phenol, bisphenol A (BPA), L-phenylalanine (Phe), L-tyrosin (Tyr), anhydrous ferric chloride ($FeCl_3$) and 1-chlorobutane (CB) were purchased from Aladdin Chemistry Co., Ltd. Dichloroethane (DCE) was obtained from Fuyu Chemical Reagent Co., Ltd. (Tianjin, China). Other solvents are of analytical grade.

Synthesis of Hypercrosslinked Polymers

Hypercrosslinked polymers were obtained by Friedel-Crafts addition polymerization of DVB itself or the mixture of DVB and other aromatic units in the presence of anhydrous $FeCl_3$. In a typical synthesis, 1.84 g of DVB and 0.46 g of monomers (DVB/monomers=4/1, *W*/*W*) were dissolved in solvents (20 mL) in ice bath and then 0.55 g of $FeCl_3$ was added to the solution. The resulting mixture was heated to 80 °C for 24 h. After being cooled down to room temperature, the solid products were washed by ethanol to remove the solvent and other components. Then, the products were soaked in 100 mL of 1 mol/L hydrochloric acid for overnight. Finally, the products were washed with water until the washing solution is neutral and then dried in an oven at 50 °C until constant weight. The yield of the polymer is defined as the ratio of the total weight of monomer and crosslinker to the weight of the dried product.

As control, PDVB particles were obtained by radical polymerization under similar conditions except that AIBN was used as radical initiator according to the previous study.[46] Briefly, DVB (4.36 mL), AIBN (8 wt% relative to monomers), and acetonitrile (25.6 mL) were added in a teflonlined stainless-steel autoclave. After polymerization at 85 °C for 4 h, the particles were separated and washed by methanol over a G-5 sintered glass filter, and then dried till constant weight.

Characterization

Fourier transform infrared (FTIR, Spectrum One; PerkinElmer, Waltham, MA) spectroscopy was used to analyze the structures of the samples in KBr disc in the range of 400–4000 cm^{-1}. The content of the residual double bonds can be determined by infrared spectroscopy according to the literature with a slight modification.[47] The residual double bond content (C_{rvg}) is roughly estimated from the following equations:

$$X_{vb} = \frac{(A + B)}{2(C + D)} \times 100\% \quad (1)$$

$$C_{rvg} = C_{vg} \times X_{vb} \quad (2)$$

where X_{vb} is the percentage of residual double bond content; C_{vg} represents the vinyl content of DVB, 15.4 mmol/g; A, B, C and D are the unit of Kubelka-Munk (K-M) multiplied by the peak value of the corresponding extinction coefficient height, where the vinyl bands are assigned at both 1630 cm^{-1} (A) and 990 cm^{-1} (B); the characteristic bands corresponding to the substituted benzene ring are at both 1510 cm^{-1} (C) and 795 cm^{-1} (D).

X-ray photoelectron spectroscopy (XPS) was used to analyze the structure of samples on Thermo ESCALAB 250XI (Waltham, Massachusetts, America). Bruker Avance II 400 WB 600 MHz spectrometer (Bruker Switzerland AG) was used to record solid state ^{13}C cross-polarized magic angle rotation (CP/MAS) NMR spectra of the samples. The images of scanning electron microscopy (SEM) were obtained by Carl Zeiss GeminiSEM300 (Oberkochen, Germany). The dried samples were sprayed with gold before the test. The nitrogen adsorption-desorption isotherms were collected by pore size analyzer Micromeritics ASAP 2020 M (Micromeritics, Norcross, GA) in a nitrogen bath (77 K) with 99.999% purity of nitrogen. Before the experiment, a known quantity of the samples was degassed in vacuum at 110 °C for 8 h. The hydrogen (H_2) adsorption isotherms were determined on a Micromeritics 3 Flex instrument (Micromeritics, America) at 77.3 K. The thermal properties of the samples were obtained using a Diamond TG/DTA (PerkinElmer, Shanghai, China) by heating each sample from 25 °C to 850 °C with a heating rate of 20 °C/min under nitrogen atmosphere. Water contact angle measurements were

https://doi.org/10.1007/s10118-022-2667-7

conducted on an instrument (OCA 40, Dataphysics, Germany) at room temperature according to literature.[45] Before tests, HCPs products were ground using a pestle and mortar and then removed larger particles by a 300-mesh sieve.

RESULTS AND DISCUSSION

Selection of Solvent

Solvent plays a vitally important role in controlling the morphology and pore size distribution of porous polymers.[48,49] However, there are few investigations on solvent effect on HCPs as dichloroethane was generally chosen as the default option. In this work, we adopted various solvents with different polarity and solvation to DVB for fabrication of HCPDVB. High yields of solid products can be obtained in most used solvents except DMSO, isopropyl alcohol and cyclohexanone, while the products have high surface areas only when dichloroethane or 1-chlorobutane is used (Table S1 in the electronic supplementary information, ESI, and Fig. 1). Our results are significantly different from that reported in the research for post-crosslinking of poly(divinylbenzene-*co*-vinylbenzyl chloride) (DVB-VBC) precursors,[50] but much similar to that observed in the investigation on self-condensation of dichloroxylene.[51] In the first case, Sherrington and co-workers found that a poor solvent (*e.g.*, hexane) of polystyrene (PS) can also yield a high surface area (~600 m^2/g); by contrast, in the

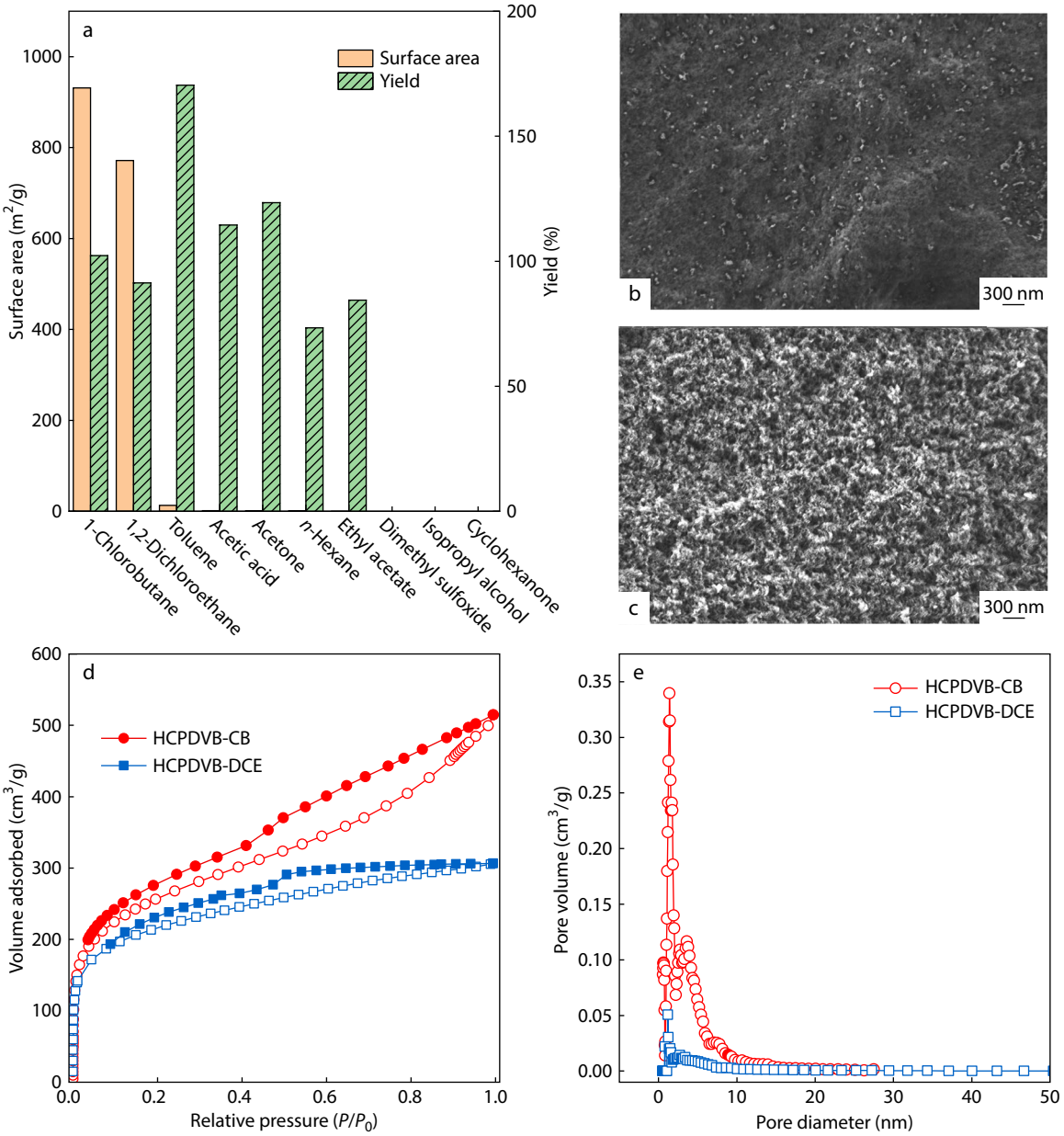

Fig. 1 (a) Effect of solvent on preparation of HCPDVB; SEM images of polymers prepared in (b) dichloroethane (HCPDVB-DCE) and in (c) 1-chlorobutane (HCPDVB-CB), respectively. Nitrogen adsorption (open) and desorption (solid) isotherms (d) at 77 K and pore size distribution (e) based on DFT calculation of HCPDVB-DCE and HCPDVB-CB, respectively.

https://doi.org/10.1007/s10118-022-2667-7

second case, Liu *et al.* observed that only choloro-containing solvent (DCE or 1,1,2-trichloroethane) can achieve surface area of HCPs greater than 100 m^2/g. In principle, an appropriate solvent is a thermodynamically good solvent for polymer precursor/monomer, and is compatible with Friedel-Crafts chemistry, simultaneously. By comparing the difference of solvents in Hansen three-dimensional parameter (Table S1 in ESI), it is difficult to give a unified explanation for the effect of individual solvent. Firstly, given DMSO or isopropyl alcohol with a greater δ_h that is related to hydrogen bonding, possibly meaning that the carbonate intermediate is unsteady in such hydrogen-bonding acceptor solvents. As a result, the self-polymerization of DVB is prevented. Secondly, the yields of HCPDVB products sometimes achieve greater than 100% (Fig. 1a). These phenomena were also observed in fabrication of other HCPs. For an example, two self-condensations of 1,4-benzenedimethanol and benzyl alcohol achieved 120% and 115% yields of the corresponding HCPs, respectively.[24] Such phenomena may be possibly attributed to the difficulty in complete removal of iron residues within the networks.[52] Thirdly, the effect of the used solvents on polymerization could account for the difference in polymer yield. In view of the difference in solvation to polymer and compatibility with F-C reaction, the solvents used can be classified into four groups (Table S2 in ESI). In our cases, when the solvent is favorable for both factors: DCE or CB (type I), high yields are obtained; when the solvent is not compatible with F-C reaction, *e.g.*, DMSO (type II) or isopropyl alcohol (type III), no products can be found; when the solvent has a good compatibility with F-C reaction but poor solvation to polymer, *e.g.*, acetic acid or acetone (type IV), greater yields are observed. Additionally, toluene is a special solvent under the conditions used. Due to its aromatic ring, toluene actually plays a dual role in the polymerization, *i.e.*, solvent and building block (monomer). This will lead to a greater yield of the polymer than the theoretical one because of without considering solvent contribution. Nevertheless, there are still some contradictions, and thus more investigations on effect of solvent are undoubtedly necessary in the future study.

Morphology and pore characteristic of HCPDVB were evaluated by SEM and nitrogen adsorption. From the SEM images shown in Fig. 1, irregular nanoparticles are accumulated into bulk solid. In comparison with a dense structure observed in HCPDVB-DCE prepared in DCE (Fig. 1b), a loose structure can be observed in HCPDVB-CB obtained in 1-chlorobutane (Fig. 1c). Derived from nitrogen adsorption (Fig. 1 and Table 1), HCPDVB-CB is tested to achieve 931 m^2/g of surface area when 1-chlorobutane was used as solvent, while HCPDVB-DCE has 771 m^2/g of surface area when DCE was used as solvent. Nitrogen adsorption-desorption isotherms of HCPDVB-DCE and HCPDVB-CB are shown in Fig. 1(d). A steep rise at relatively low pressure (P/P_0<0.01) is found in the two isotherms, demonstrating that the two polymers have abundant microporous structures. A hysteresis loop at medium pressure (P/P_0=0.4–0.7) is also found in both isotherms, suggesting the existence of mesoporous. Such hierarchical porous structures could also be confirmed by the pore size distribution (Fig. 1e). Notably, micropore contribution in HCPDVB-CB is significantly greater than that in HCPDVB-DCE, indicating that chlorobutane is a better choice for obtaining high surface area under the conditions used. These results could be responsible for the better compatibility between chlorobutane and DVB80 than that between DCE and DVB80, as the solubility parameter of chlorobutane (17.2 $MPa^{1/2}$) is much closer to that of DVB80 (18.1 $MPa^{1/2}$) compared to that of DCE (20.8 $MPa^{1/2}$).

Other effects on yield and surface area of polymer were also investigated (Table S3 in ESI). The catalyst amount largely affects the polymerization process. With an increase in catalyst content, the polymerization rapidly yields high polymer content and maintains complete transformation when $FeCl_3$ content is equal or above 10 wt%. Meanwhile, the surface area displays a bell shape change, and the highest surface area is achieved when $FeCl_3$ content is in the range of 10 wt%–20 wt%. This is distinctively different from most reports on fabrication of HCPs, in which a great consumption of catalyst is needed, normally two-fold greater than precursors weight. Additionally, the reaction temperature was also found to have a significant effect on surface area of polymer. In comparison with room temperature, a higher reaction temperature (80 °C) brought about around six-fold increase in surface area. This is in accordance with the mechanism of step-growth polymerization but much different from that of ionic polymerization.

Mechanism of Friedel-Crafts Addition Polymerization of DVB

These phenomena above stimulated us to find a reasonable understanding to explain how DVB polymerizes in the presence of Lewis acid. Since Heuer and Staudinger reported the synthesis of polymerization of styrene-DVB initiated by radical initiator, various polymerizations of styrenes have been developed, leading to the foundation of modern polymer industry.[44] It is well known that styrenes are very prone to free radical polymerization as well as ionic polymerization dependent on reaction conditions. In numerous literature on the preparation of HCPs, DVB usually first polymerizes with styrene by free radical polymerization to form a precursor that can be further intercrosslinked by crosslinkers. The polymerization in this case normally involves the reaction between the double bonds on the side chains. In practice, the second double bond of DVB has relatively low reactivity, and is thus difficult to react completely, resulting in polymers of low crosslinking

Table 1 Porosity properties of HCPDVB-CB and HCPDVB-DCE obtained by Friedel-Crafts addition polymerization.

Sample	S_{BET} [a] (m^2/g)	S_{micro} [b] (m^2/g)	PV [c] (cm^3/g)	MPV [d] (cm^3/g)	Micropore ratio [e] (%)	Average pore size (nm)
HCPDVB-CB	931	412	0.72	0.18	44.3	3.4
HCPDVB-DCE	771	198	0.56	0.11	25.7	2.9

[a] BET surface area calculated from nitrogen adsorption isotherms at 77.3 K using the BET equation. [b] Micropore surface area calculated from nitrogen adsorption isotherms at 77.3 K using the *t*-plot equation. [c] Pore volume calculated from the nitrogen isotherm at P/P_0 = 0.99, 77.3 K. [d] Micropore volume calculated from the nitrogen isotherm at P/P_0 = 0.15, 77.3 K using the *t*-plot equation. [e] Surface area ratio of micropore surface area to the total BET surface area.

https://doi.org/10.1007/s10118-022-2667-7

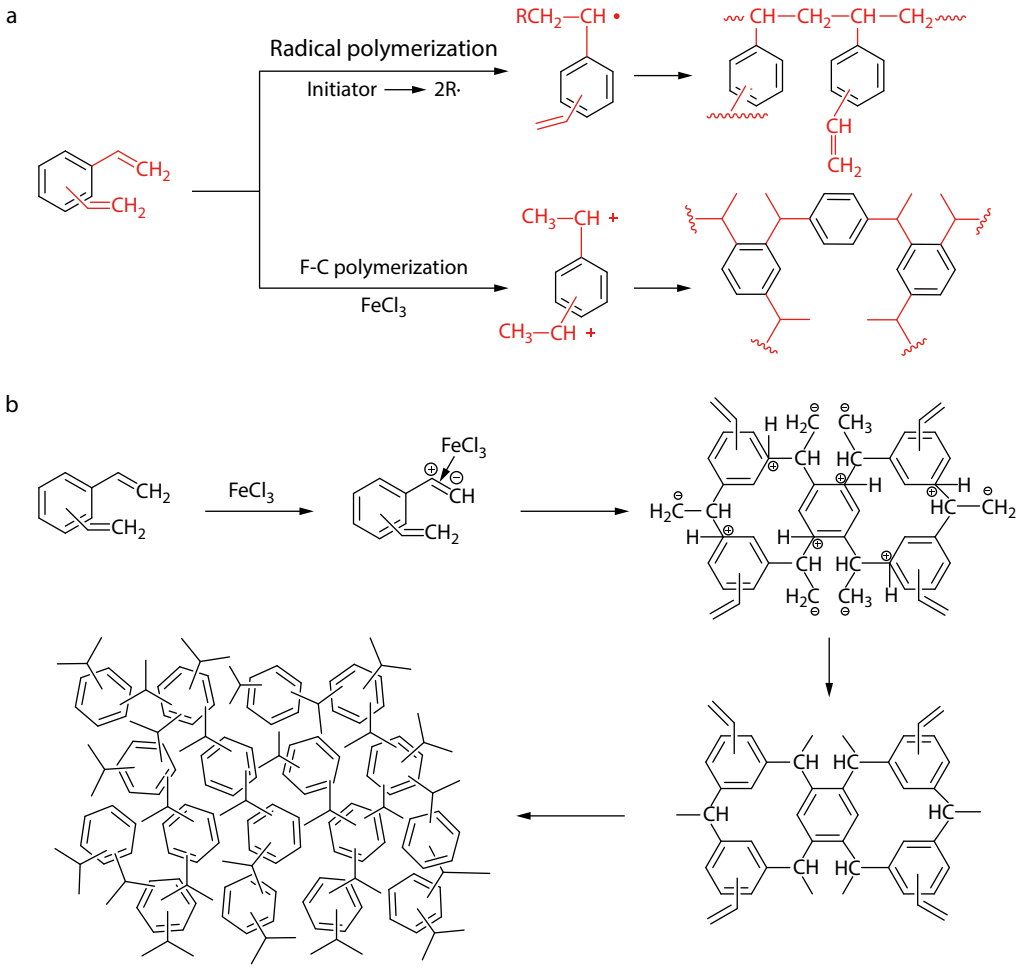

Fig. 2 Comparison of polymerization mechanism of DVB by radical polymerization and by Friedel-Crafts addition polymerization.

degree (Fig. 2a). By contrast, in our case, we speculate that the double bonds on DVB are rearranged onto benzyl carbocation with methyl under the catalysis of Lewis acid, and then connected with benzene ring of another DVB molecule to form an extensive crosslinked network (Fig. 2b). The arrangement of benzyl rings of the polymers is the main difference in the polymer structures between the two polymerization reactions. The backbone of the polymer is composed of the benzyl rings under Friedel-Crafts reaction, while it consists of alkyl chain with the benzyl rings locating in the side chains of the polymer under radical polymerization.[40]

By comparing the FTIR spectra of samples shown in Fig. 3(a), the structure change in polymerization of divinyl benzene can be observed. The most obvious change is the disappearance of the double bond at 1630 cm^{-1}, which proves the occurrence of reaction. Friedel-Crafts reactions achieve greater than 99% double bond conversion, while radical polymerization leads to 26.4% double bond left in the matrix (Table S4 in ESI). This result strongly confirmed that Friedel-Crafts reaction possesses much higher reactivity compared with radical polymerization, which is similar to the phenomenon observed in the post-crosslinking reaction of PDVB.[40] Another difference from PDVB particles obtained by radical polymerization, HCPDVB networks show complex peaks at around 3000 cm^{-1} that is the characteristic spectra of the Friedel-Crafts reaction, indicating that polysubstitution occurs on the benzene ring.[53] The band at 854 cm^{-1} represents the vibration of C—H band in the benzene ring with *para*-functional groups, and the band decreases after the reaction, further confirming the formation of the hypercrosslinked structure.[50]

Solid-state ^{13}C CP/MAS NMR spectroscopy was used to further analyze the chemical structures of networks, as shown in Fig. 3(b). Three main peaks of the spectra were observed at 39, 125 and 139 ppm, corresponding to the methine crosslinked point, the non-substituted aromatic carbons, and the substituted aromatic carbons, respectively (Table S5 in ESI). The peak at 20 ppm is a significant mark of methyl, which, together with the peak at 39 ppm, confirmed the rearrangement in the Friedel-Crafts reaction of DVB. As we hypothesized, the double bonds on DVB were rearranged onto benzyl carbocation with methyl under the catalysis of Lewis acid, and then crosslinked with benzene ring of another molecule to form a hypercrosslinked network. The formed structures tend to be polysubstituent, as indicated by wide peaks at 125 and 139 ppm.[53,54] Notably, the two peaks at 112 and 137 ppm corresponding to double bond were observed in HCPDVB-ACN but almost disappeared in HCPDVB-CB, HCPDVB-DCE and HCPDVB-EAC, which further confirmed the effect of

https://doi.org/10.1007/s10118-022-2667-7

solvent on polymerization reaction. Additionally, the appearances of the peaks at above 180 ppm and their symmetrical peaks could be possibly attributed to spinning side bands caused by instruments.[33,53,54]

XPS analysis indicates that three types of carbon bond are clearly found in the C 1s spectra of HCPDVB products (Figs. 3c and 3d). The peaks at 285.4, 285.0, and 284.4 eV correspond to carbon-oxygen bond, carbon-carbon bond, and carbon-carbon double bond, respectively. The peak at 285.4 eV is possibly caused by combining with the water in the air.[55] There is no difference of carbon bond type in between HCPDVB-CB and HCPDVB-DCE. Thermal gravity curves derived from TGA analysis show that HCPDVB polymer has a higher initial decomposition temperature (400 °C) than that (350 °C) observed for PDVB obtained by radical polymerization (Fig. 3e), possibly because the extensive crosslinked HCPDVB has more rigid structure, leading to the greater heat-resistance.

DVB as External Crosslinker

In addition to the ability for self-addition polymerization, the presence of two double bond on DVB allows for its use as a new type of external crosslinker for HCPs. Unlike common

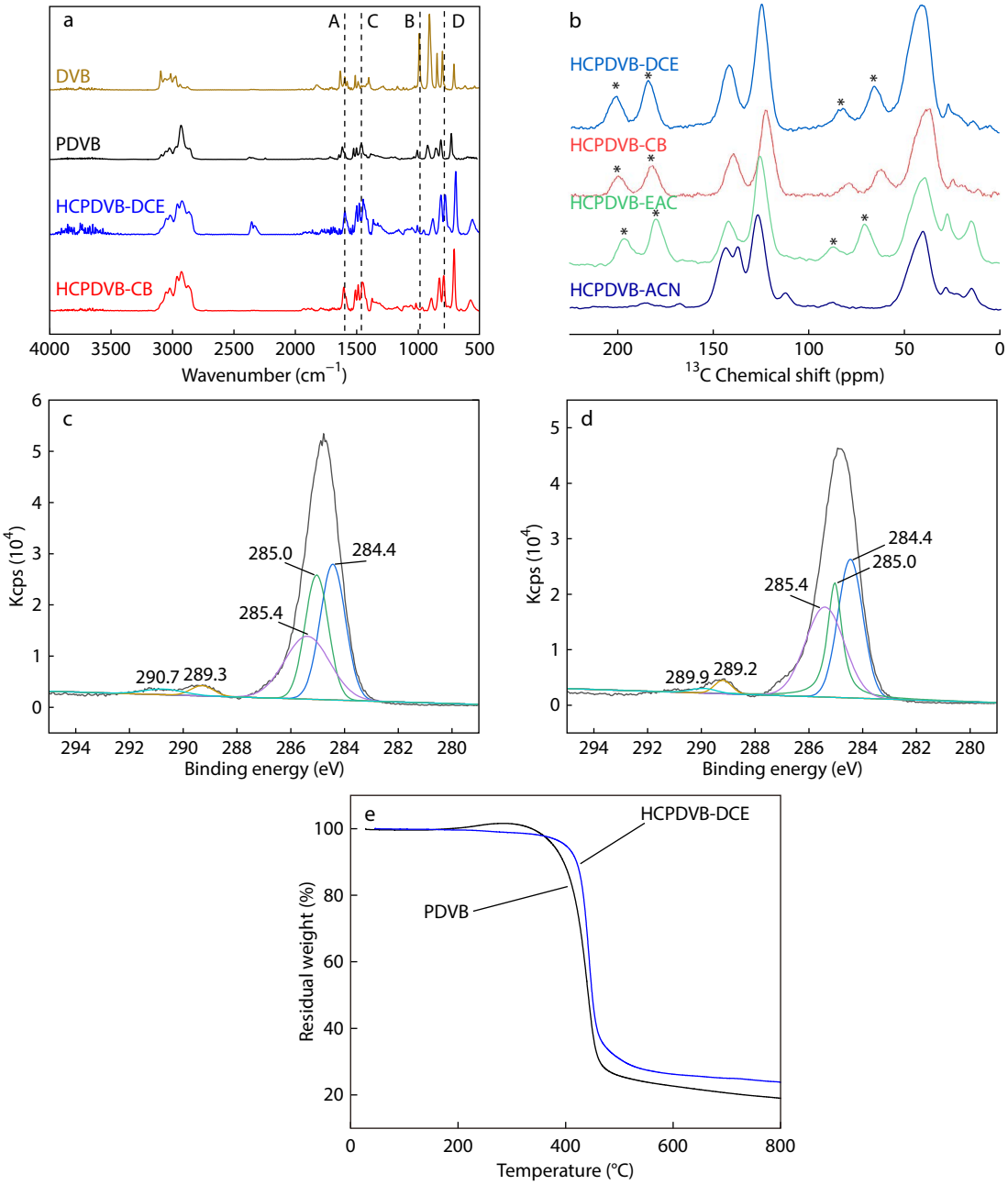

Fig. 3 FTIR spectra (a) and ^{13}C CP/MAS NMR spectra (b) of monomer and polymers, * represents spinning side bands. High resolution C 1s XPS spectra of HCPDVB-DCE (c) and HCPDVB-CB (d); TGA curves of PDVB obtained by radical polymerization and HCPDVB-DCE obtained by Friedel-Crafts addition polymerization (e).

https://doi.org/10.1007/s10118-022-2667-7

crosslinkers based on condensation reactions, the double-bond crosslinker results in free of byproduct. Traditionally, HCPs are intrinsic hydrophobicity as the starting materials, including precursor, monomer, and crosslinker, are all hydrophobic molecules. It is normally believed to be difficult to obtain hydrophilic HCPs by one-step polymerization.[54,56] To investigate the superiority of DVB as external crosslinker, we chose phenol, bisphenol A,L-phenylalanine and L-tyrosine as polar aromatic units to copolymerize with DVB. The possible Friedel-Crafts copolymerization processes are illustrated in Fig. 4 according to the proposed mechanism in this study.

The surface morphology of the copolymers was observed by SEM (Fig. S2 in ESI). The similar morphology was found in both HCP(BPA-DVB) and HCP(Phe-DVB) to that of HCPDVB-CB. In the FTIR spectra of copolymers (Fig. 5a), the disappearance of the double bond at 1630 cm^{-1} is also observed. The band near 3300 cm^{-1} is attributed to O—H or N—H stretching vibration, and the band near 1744 cm^{-1} corresponds to C=O, which are absent in the spectra of HCPDVB products, indicating the successful linking of polar aromatic molecules to DVB. As same as HCPDVB, both HCP(BPA-DVB) and HCP(Phe-DVB) show resonance peaks near 139 and 120 ppm in ^{13}C CP/MAS NMR spectra (Fig. 5b), which are possibly attributed to the substituted aromatic carbon and the non-substituted aromatic carbon, respectively. The peak at 20 ppm attributed to methyl further confirmed the similar reaction mechanism of polymerization of polar aromatic molecules with DVB to that of self addition of DVB. Figs. 5(c)–5(f) show the full dataset and the wide range of C environments for XPS characterization of samples. The products mainly consist of carbon and oxygen, and HCP(Phe-DVB) contains a few amounts of N element when phenylalanine was used as monomer (Fig. S3 in ESI). The signal of aromatic sp^2 carbon (284.3 eV) is obvious, and the peak at 285.0 eV is caused by the aliphatic carbon groups which are the connection units of benzenes. The peak at 285.6 eV represents C—O carbons of partial monomers, possibly derived from the combined water in the air as well as from carboxyl group on Phe. The peak at 289.8 eV corresponds to C—CO_3, which could be attributed to the combination of CO_2 in air according to the description by Robshaw and co-workers.[57] Energy dispersive spectrometer (EDS) was used for the elemental determination of HCP(BPA-DVB) and HCP(Phe-DVB) (Figs. 5g and 5h). A large amount of C and O are observed in HCP(BPA-DVB) and HCP(Phe-DVB), and a small amount of N is found in HCP(Phe-DVB), indicating that the polar aromatic molecules successfully copolymerized with DVB. As shown in Fig. S4 and Table S6 (in ESI), after copolymerization of DVB and polar aromatic compounds, water contact angles decreased from 146.2° to 107.5°, to some extent, showing an improvement on hydrophilicity of copolymers. The fall ranges of WCAs seem not to be solely dependent on the solubility of the polar aromatic compound in water.

Nitrogen sorption isotherms were used to further study the porous properties of copolymers (Fig. 6 and Table 2). A combination of Type I and Type IV isotherm characteristics of isotherms is also observed in all the four copolymers. The relatively abundant microporous and mesoporous structures were found in the products, but the total surface area of the copolymers decreased compared to that of HCPDVB, possibly because the addition of nucleophilic aromatic units reduced the activity of Friedel-Crafts alkylation. In comparison with bisphenol A, phenol molecule has one more substitute active site on the phenyl ring, possibly resulting in greater micropores of HCP(Phenol-DVB) than those of HCP(BPA-DVB). A similar phenomenon was observed in HCP(Phe-DVB) and HCP(Tyr-DVB). The micropore surface area of HCP(Phe-DVB) is about 18 times larger than that of HCP(Tyr-DVB). Another factor affecting F-C reactivity is molecular electrophilicity. Compared to phenol and L-tyrosin, bisphenol A and L-phenylalanine have higher electronic cloud density on phenyl rings, probably leading to higher F-C reactivity. Combined with the two factors, HCP(BPA-DVB) and HCP(Phe-DVB) display greater surface areas than HCP(Phenol-DVB) and HCP(Tyr-DVB).

We further tested the effect of functional monomer on H_2 adsorption performance of the polymers. HCPDVB-CB obtained by self-polymerization of DVB was composed of carbon and hydrogen atoms, and achieved 0.30 wt% of H_2 uptake. After the addition of oxygen-rich molecule (bisphenol A) and oxygen/nitrogen-rich molecule (L-phenylalanine), the H_2 adsorption of the copolymers shows a significant improve-

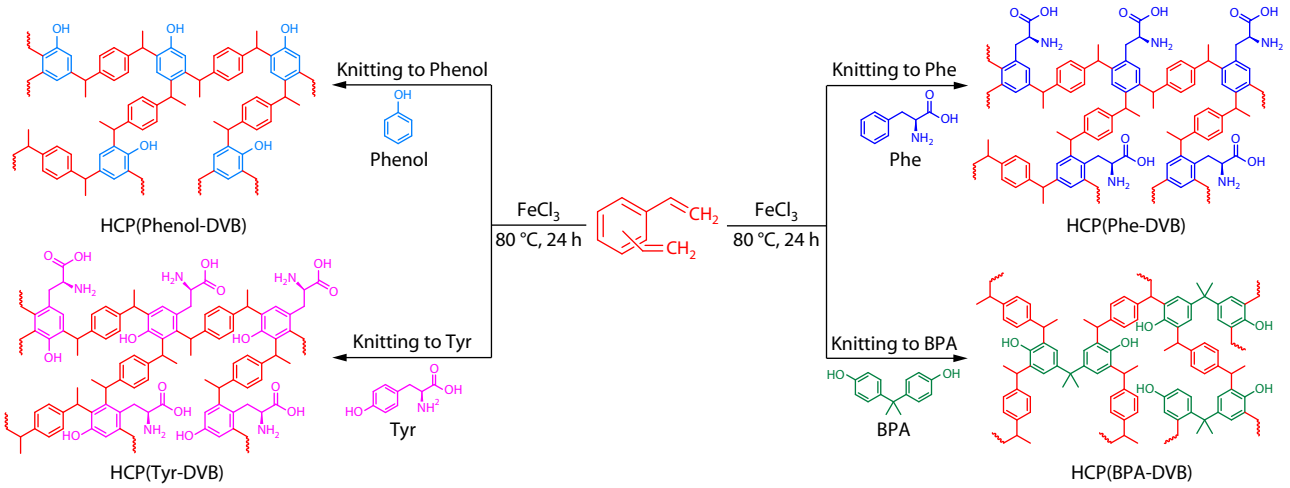

Fig. 4 Synthesis of hypercrosslinked polymers by DVB-knitting *via* Friedel-Crafts addition polymerization.

https://doi.org/10.1007/s10118-022-2667-7

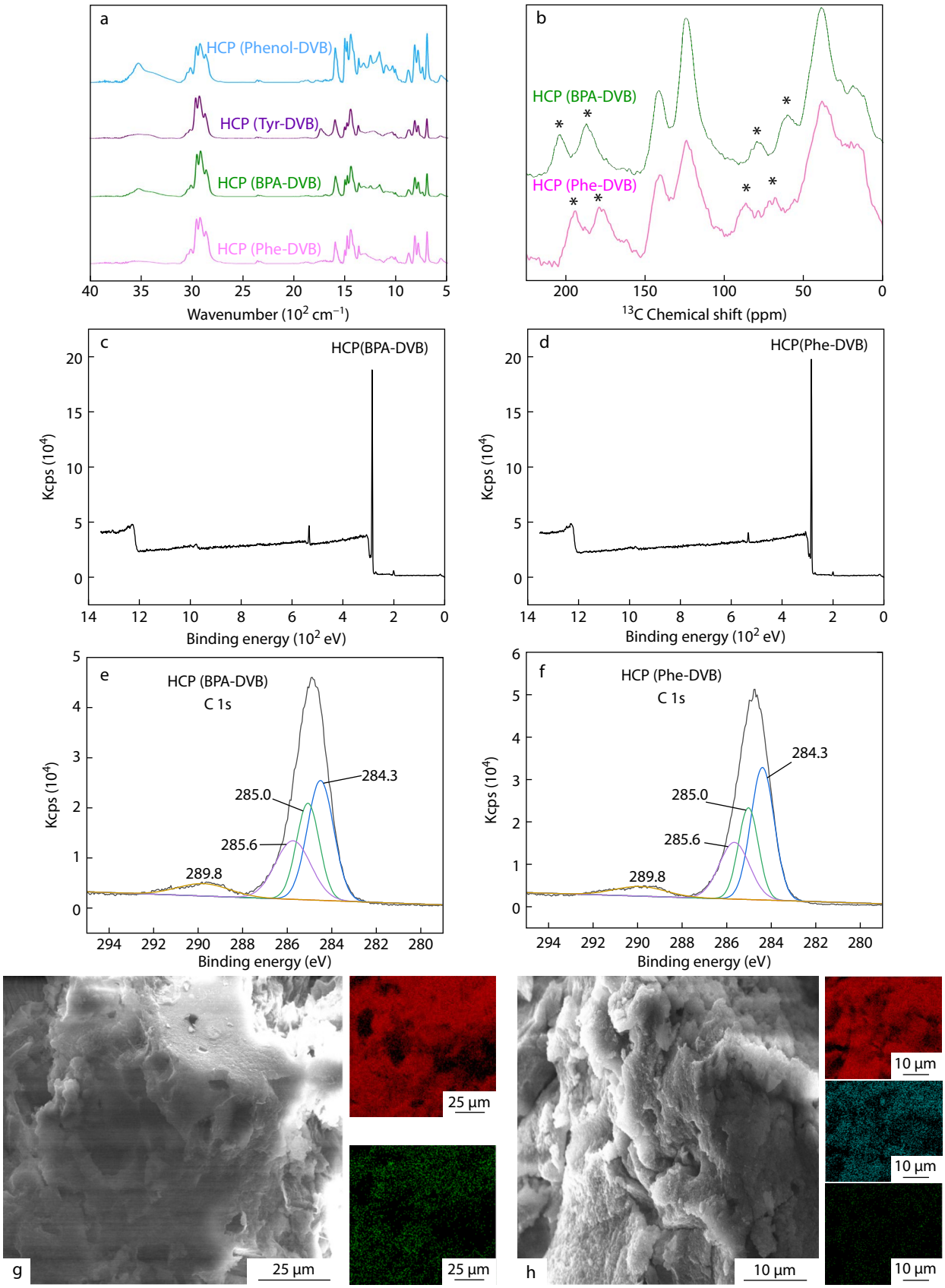

Fig. 5 FTIR spectra (a) and ^{13}C CP/MAS NMR spectra (b) of HCPs obtained by DVB knitting, * represents spinning side bands. X-ray photoelectron spectroscopy survey spectra and high-resolution C 1s XPS spectra of HCP(BPA-DVB) (c, e) and HCP(Phe-DVB) (d, f), respectively. EDS mappings of HCP(BPA-DVB) (g) and HCP(Phe-DVB) (h).

https://doi.org/10.1007/s10118-022-2667-7

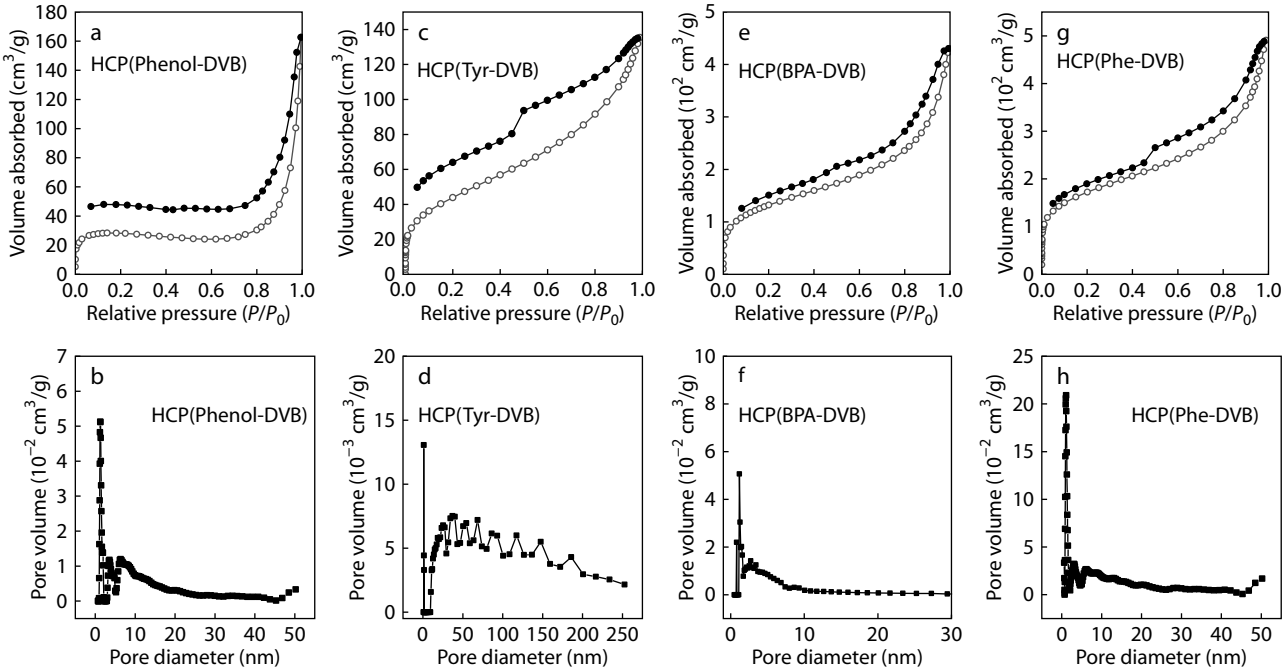

Fig. 6 Nitrogen adsorption (open) and desorption (solid) isotherms at 77 K and pore size distribution based on DFT calculation of HCP(Phenol-DVB) (a b) and HCP(Tyr-DVB) (c, d), HCP(BPA-DVB) (e, f) and HCP(Phe-DVB) (g, h).

Table 2 Porosity properties of the HCPs obtained by DVB-knitting.

Sample	S_{BET} [a] (m^2/g)	S_{micro} [b] (m^2/g)	PV [c] (cm^3/g)	MPV [d] (cm^3/g)	Micropore ratio [e] (%)	Average pore size (nm)
HCP(Phenol-DVB)	113	113	0.25	0.04	100.0	33.8
HCP(Tyr-DVB)	161	12	0.21	0	7.5	3.06
HCP(BPA-DVB)	477	77	0.66	0.03	16.1	5.93
HCP(Phe-DVB)	612	218	0.76	0.01	35.6	3.42

The weight ratio of crosslinker to monomer was fixed at 4/1, and the weight ratio of catalyst to monomer was 3/1 in all recipes. [a] BET surface area calculated from nitrogen adsorption isotherms at 77.3 K using the BET equation. [b] Micropore surface area calculated from nitrogen adsorption isotherms at 77.3 K using the *t*-plot equation. [c] Pore volume calculated from the nitrogen isotherm at P/P_0=0.99, 77.3 K. [d] Micropore volume calculated from the nitrogen isotherm at P/P_0=0.15, 77.3 K using the *t*-plot equation. [e] Volume ratio of micropore volume to the total pore volume.

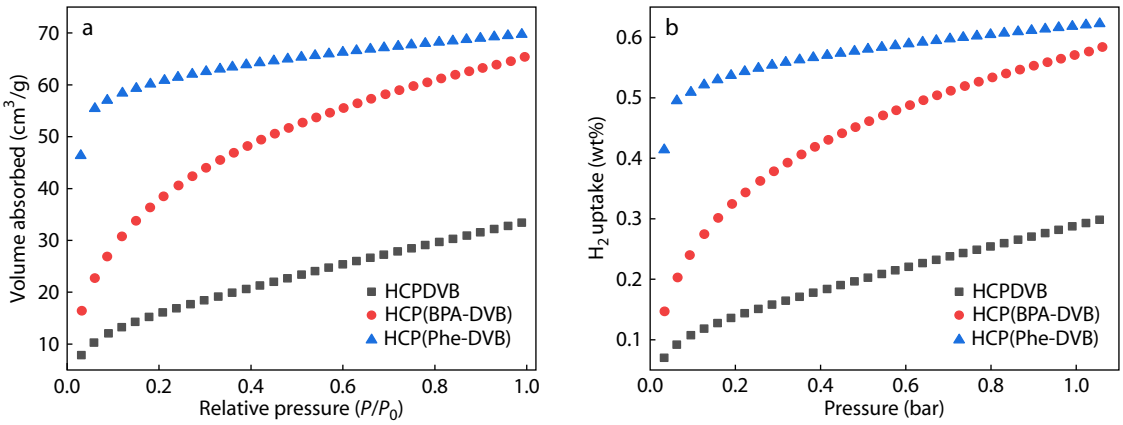

Fig. 7 H_2 adsorption isotherms of HCPDVB-CB, HCP(BPA-DVB) and HCP(Phe-DVB) at 77 K.

ment, reaching 0.58 wt% of H_2 uptake for HCP(BPA-DVB) and 0.62 wt% of H_2 uptake for HCP(Phe-DVB), respectively (Fig. 7). The novel copolymers have comparable hydrogen storage with POSS-based HCPs,[41,58] and relatively lower than recent heteroatom-based HCPs.[59,60] However, given that DVB and amino acids are easily available, especially and that amino acids are chiral molecules, the resultant HCPs knitted by DVB are believed to find more applications, such as chiral separation, enzyme immobilization, drug delivery, and so on.

CONCLUSIONS

In summary, an environmentally and atom-economically benign process was provided to fabricate hypercrosslinked

polymers by self-addition polymerization of divinyl benzene and its knitting to polar aromatic molecules. 1-Chlorobutane, a compound with a single chlorine atom, was used as solvent and proven to be a better alternative than 1,2-dichloroethane in the F-C reaction. The surface area of HCPDVB obtained by self-addition polymerization of DVB can reach 931 m^2/g without removing harmful small molecules. Additionally, the ability of DVB as a novel double-bonded small molecule crosslinker was demonstrated for knitting polar aromatic compounds by F-C reaction to form hypercrosslinked networks. The HCP(Phe-DVB) and HCP(BPA-DVB) prepared using phenylalanine and bisphenol A as functional monomers can obtain 612 m^2/g and 471 m^2/g, respectively. These products containing nitrogen and oxygen rich component could improve their hydrogen storage than HCPDVB. Based on the advantages of the addition reaction, the proposed process to produce HCPs with high atom efficiency is expected to find a wide range of applications.

NOTES

The authors declare no competing financial interest.

Electronic Supplementary Information

Electronic supplementary information (ESI) is available free of charge in the online version of this article at http://doi.org/10.1007/s10118-022-2667-7.

ACKNOWLEDGMENTS

The authors gratefully thank National Key R&D Program of China (No. 2017YFC1600404) and Natural Science Foundation of Shandong Province (No. ZR2013BM011) for financial support. The work was also supported by Open Projects Fund of Shandong Key Laboratory of Carbohydrate Chemistry and Glycobiology, Shandong University (No. 2019CCG02), Shandong Key Laboratory of Fluorine Chemistry and Chemical Engineering Materials, and Science and Technology Bureau of Jinan (No. 2021GXRC105). The authors thank Dr. Yang Xu for valuable discussion with preparation and characterization of HCPs.

REFERENCES

1 Zhu, J. Y.; Yuan, S. S.; Wang, J.; Zhang, Y. T.; Tian, M. M.; Bruggen, B. V. Microporous organic polymer-based membranes for ultrafast molecular separations. *Prog. Polym. Sci.* **2020**, *110*, 101308.
2 Du, M. Q.; Peng, Y. Z.; Ma, Y. C.; Yang, L.; Zhou, Y. L.; Zeng, F. K.; Wang, X. K.; Song, M. L.; Chang, G. J. Selective carbon dioxide capture in antifouling indole-based microporous organic polymers. *Chinese J. Polym. Sci.* **2020**, *38*, 187–194.
3 Das, S.; Heasman, P.; Ben, T.; Qiu, S. L. Porous organic materials: strategic design and structure-function correlation. *Chem. Rev.* **2017**, *117*, 1515–1563.
4 Côté, A. P.; Benin, A. I.; Ockwig, N. W.; O'Keeffe, M.; Matzger, A. J.; Yaghi, O. M. Porous, crystalline, covalent organic frameworks. *Science* **2005**, *310*, 1166–1170.
5 Hu, X. L.; Li, H. G.; Tan, B. E. COFs-based porous materials for photocatalytic applications. *Chinese J. Polym. Sci.* **2020**, *38*, 673–684.
6 Wang, M. Y.; Zhang, Q. J.; Shen, Q. Q.; Li, Q. Y.; Ren, S. J. Truxene-based conjugated microporous polymers *via* different synthetic methods. *Chinese J. Polym. Sci.* **2020**, *38*, 151–157.
7 Lei, Y.; Tian, Z. Y.; Sun, H. X.; Liu, F.; Zhu, Z. Q.; Liang, W. D.; Li, A. Low-resistance thiophene-based conjugated microporous polymer nanotube filters for efficient particulate matter capture and oil/water separation. *ACS Appl. Mater. Interfaces* **2021**, *13*, 5823–5833.
8 Kuhn, P.; Antonietti, M.; Thomas, A. Porous, covalent triazine-based frameworks prepared by ionothermal synthesis. *Angew. Chem. Int. Ed.* **2008**, *47*, 3450–3453.
9 Kamiya, K. Selective single-atom electrocatalysts: a review with a focus on metal-doped covalent triazine frameworks. *Chem. Sci.* **2020**, *11*, 8339–8349.
10 Ben, T.; Ren, H.; Ma, S. Q.; Cao, D. P.; Lan, J. H.; Jing, X. F.; Wang, W. C.; Xu, J.; Deng, F.; Simmons, J. M.; Qiu, S. L.; Zhu, G. S. Targeted synthesis of a porous aromatic framework with high stability and exceptionally high surface area. *Angew. Chem. Int. Ed.* **2009**, *48*, 9457–9460.
11 Shen, Y. M.; Xue, Y.; Yan, M.; Mao, H. L.; Cheng, H.; Chen, Z.; Sui, Z. W.; Zhu, S. B.; Yu, X. J.; Zhuang, J. L. Synthesis of TEMPO radical decorated hollow porous aromatic frameworks for selective oxidation of alcohols. *Chem. Commun.* **2021**, *57*, 907–910.
12 Jung, D.; Chen, Z. J.; Alayoglu, S.; Mian, M. R.; Goetjen, T. A.; Idrees, K. B.; Kirlikovali, K. O.; Islamoglu, T.; Farha, O. K. Postsynthetically modified polymers of intrinsic microporosity (PIMs) for capturing toxic gases. *ACS Appl. Mater. Interfaces* **2021**, *13*, 10409–10415.
13 Tozawa, T.; Jones, J. T. A.; Swamy, S. I.; Jiang, S.; Adams, D. J.; Shakespeare, S.; Clowes, R.; Bradshaw, D.; Hasell, T.; Chong, S. Y.; Tang, C.; Thompson, S.; Parker, J.; Trewin, A.; Bacsa, J.; Slawin, A. M. Z.; Steiner, A.; Cooper, A. I. Porous organic cages. *Nat. Mater.* **2009**, *8*, 973–978.
14 Webstet, O. W.; Gentry, F. P.; Farlee, R. D.; Smart, B. E. Hypercrosslinked rigid-rod polymers. *Makromol. Chem. Macromol. Symp.* **1992**, *54*, 477–482.
15 Li, J. Q.; Wang, Z.; Wang, Q. Q.; Guo, L. Y.; Wang, C.; Wang, Z.; Zhang, S. H.; Wu, Q. H. Construction of hypercrosslinked polymers for high-performance solid phase microextraction of phthalate esters from water samples. *J. Chromatogr. A* **2021**, *1641*, 461972.
16 Fontanals, N.; Marcé, R. M.; Borrulla, F.; Cormack, P. A. G. Hypercrosslinked materials: preparation, characterisation and applications. *Polym. Chem.* **2015**, *6*, 7231–7244.
17 Tan, L. X.; Tan, B. E. Hypercrosslinked porous polymer materials: design, synthesis, and applications. *Chem. Soc. Rev.* **2017**, *46*, 3322–3356.
18 Tan, L. X.; Tan, B. E. Research progress in hypercrosslinked microporous organic polymers. *Acta Chimica Sinica* (in Chinese) **2015**, *73*, 530–540.
19 Davankov, V.; Tsyurupa, M.; Ilyin, M.; Pavlova, L. Hypercross-linked polystyrene and its potentials for liquid chromatography: a mini-review. *J. Chromatogr. A* **2002**, *965*, 65–73.
20 Davankov, V. A.; Rogozhin, S. V.; Tsyurupa, M. P.; **1973**, U.S. Pat.; 3,729,457
21 Hradil, J.; Králová, E. Styrene-divinylbenzene copolymers post-crosslinked with tetrachloromethane. *Polymer* **1998**, *39*, 6041–6048.
22 Macintyre, F. S.; Sherrington, D. C.; Tetley. L. Synthesis of ultrahigh surface area monodisperse porous polymer nanospheres. *Macromolecules* **2006**, *39*, 5381–5384.
23 Wood, C. D.; Tan, B. E.; Trewin, A.; Niu, H. J.; Bradshaw, D.; Rosseinsky, M. J.; Khimyak, Y. Z.; Campbell, N. L.; Kirk, R.; Stöckel E.; Cooper, A. I. Hydrogen storage in microporous hypercrosslinked organic polymer networks. *Chem. Mater.* **2007**, *19*, 2034–2048.
24 Luo, Y. L.; Zhang, S. C.; Ma, Y. X.; Wang, W.; Tan, B. E. Microporous organic polymers synthesized by self-condensation of aromatic

hydroxymethyl monomers. *Polym. Chem.* **2013**, *4*, 1126–1131.
25 Woodward, R. T. The design of hypercrosslinked polymers from benzyl ether self-condensing compounds and external crosslinkers. *Chem. Commun.* **2020**, *56*, 4938–4941.
26 Li, B. Y.; Gong, R. N.; Wang, W.; Huang, X.; Zhang, W.; Li, H. M.; Hu, C. X.; Tan, B. E. A new strategy to microporous polymers: knitting rigid aromatic building blocks by external cross-linker. *Macromolecules* **2011**, *44*, 2410–2414.
27 Wang, S. L.; Zhang, C. X.; Shu, Y.; Jiang, S. L.; Xia, Q.; Chen, L. J.; Jin, S. B.; Hussain, I.; Cooper A. I.; Tan, B. E. Layered microporous polymers by solvent knitting method. *Sci. Adv.* **2017**, *3*, e1602610.
28 Wilson, A. S. S.; Hill, M. S.; Mahon, M. F.; Dinoi, C.; Maron, L. Organocalcium-mediated nucleophilic alkylation of benzene. *Science* **2017**, *358*, 1168–1171.
29 Gilman, H.; Meals, R. Rearrangements in the Friedel-Crafts alkylation of benzene. *J. Org. Chem.* **2002**, *8*, 126–146.
30 Rueping, M.; Nachtsheim, B. J. A review of new developments in the Friedel-Crafts alkylation from green chemistry to asymmetric catalysis. *Beilstein J. Org. Chem.* **2010**, *6*, 6.
31 Soukupová, K.; Sassi, A.; Jeřábek, K. Reinforcing of expanded polymer morphology using peroxy radical initiator. *React. Funct. Polym.* **2009**, *69*, 353–357.
32 Li, L.; Zhang, A. J.; Yu, J. H.; Li, W. Q.; Gao, H.; Tian, K.; Bai, H. One-step preparation of hierarchically porous polyureas: simultaneous foaming and hyper-crosslinking. *Polymer* **2017**, *108*, 332–338.
33 Xia, Y. X.; Di, T.; Meng, Z. H.; Zhu, T. T.; Lei, Y. J.; Chen, S.; Li, T. S.; Li, L. Versatile one-pot construction strategy for the preparation of porous organic polymers *via* domino polymerization. *Macromolecules* **2021**, *54*, 4682–4692.
34 Liu, W. H.; Wang, J. T.; Liu, J. J.; Hou, F. Y.; Wu, Q. H.; Wang, C.; Wang, Z. Preparation of phenylboronic acid based hypercrosslinked polymers for effective adsorption of chlorophenols. *J. Chromatogr. A* **2020**, *1628*, 461470.
35 Ding, L.; Zhang, A. J.; Li, W. Q.; Bai, H.; Li, L. Multi-length scale porous polymer films from hypercrosslinked breath figure arrays. *J. Colloid. Interface Sci.* **2016**, *461*, 179–184.
36 Yang, Y. W.; Tan, B. E.; Wood. C. D. Solution-processable hypercrosslinked polymers by low cost strategies: a promising platform for gas storage and separation. *J. Mater. Chem. A* **2016**, *4*, 15072–15080.
37 Ando, K.; Ito, T.; Tesehima, H.; Kusano, H.; in *Ion exchange for industry*, Ed. by Streat, M.; Springer, Chichester, UK, **1988**, p. 232–238.
38 Zeng, X. W.; Yu, T. J.; Wang, P.; Yuan, R. H.; Wen, Q.; Fan, Y. G.; Wang, C. H.; Shi, R. F. Preparation and characterization of polar polymeric adsorbents with high surface for the removal of phenol from water. *J. Hazard. Mater.* **2010**, *177*, 773–780.
39 Zeng, X. W.; Fan, Y. G.; Wu, G. L.; Wang, C. H.; Shi. R. F. Enhanced adsorption of phenol from water by a novel polar post-crosslinked polymeric adsorbent. *J. Hazard. Mater.* **2009**, *169*, 1022–1028.
40 Guo, F. H.; Wang, Y. P.; Chen, X. L.; Chen, M. Q.; He, W.; Chen, Z. Y. Supermacroporous polydivinylbenzene cryogels with high surface area: synthesis by solvothermal postcrosslinking and their adsorption behaviors for carbon dioxide and aniline. *J. Appl. Polym. Sci.* **2019**, *136*, 47716.
41 Wu, Y.; Wang, D. X.; Li, L. G.; Yang, W. Y.; Feng, S. Y.; Liu, H. Z. Hybrid porous polymers constructed from octavinylsilsesquioxane and benzene *via* Friedel-Crafts reaction: tunable porosity, gas sorption, and postfunctionalization. *J. Mater. Chem. A* **2014**, *2*, 2160–2167.
42 Shen, R.; Du, Y. J.; Yang, X. R.; Liu, H. Z. Silsesquioxanes-based porous functional polymers for water purification. *J. Mater. Sci.* **2020**, *55*, 7518–7529.
43 He, J. X.; Zhao, G. H.; Mu, P.; Wei, H. J.; Su, Y. N.; Sun, H. X.; Zhu, Z. Q.; Liang, W. D.; Li, A. Scalable fabrication of monolithic porous foam based on cross-linked aromatic polymers for efficient solar steam generation. *Sol. Energy Mater Sol. Cells* **2019**, *201*, 110111.
44 Carraher, Jr., C. E.; in *Polymer chemistry,* Marcel Dekker, New York, **2003**, p. 36–53.
45 Chen, X. L.; Ding, Y. Y.; Ren, D. Y.; Chen, Z. Y. Green synthesis of polymeric microspheres that are monodisperse and superhydrophobic, *via* quiescent redox-initiated precipitation polymerization. *RSC Adv.* **2016**, *6*, 27846–27851.
46 Huang, H. Q.; Ding, Y. Y.; Chen, X. L.; Chen, Z. Y.; Kong, X. Z. Synthesis of monodisperse micron-sized poly(divinylbenzene) microspheres by solvothermal precipitation polymerization. *Chem. Eng. J.* **2016**, *289*, 135–141.
47 Hubbard, K. L.; Finch, J. A.; Darling, G. D. The preparation and characteristics of poly(divinylbenzene-*co*-ethylvinylbenzene), including Ambetilite XAD-4. Styrenic resins with pendant vinylbenzene groups. *React. Funct. Polym.* **1998**, *36*, 17–30.
48 Okay, O. Macroporous copolymer networks. *Prog. Polym. Sci.* **2000**, *25*, 711–779.
49 Dawson, R.; Cooper, A. I.; Adams, D. J. Nanoporous organic polymer networks. *Prog. Polym. Sci.* **2012**, *37*, 530–563.
50 Ahn, J. H.; Jang, J. E.; Oh, C. G.; Ihm, S. K.; Cortez, J.; Sherrington, D. C. Rapid generation and control of microporosity, bimodal pore size distribution, and surface area in Davankov-Type hyper-cross-linked resins. *Macromolecules* **2006**, *39*, 627–632.
51 Liu, Y.; Fan, X. L.; Jia, X. K.; Zhang, B. L.; Zhang, H. P.; Zhang, A. B.; Zhang, Q. Y. Hypercrosslinked polymers: controlled preparation and effective adsorption of aniline. *J. Mater. Sci.* **2016**, *51*, 8579–8592.
52 Dawson, R.; Stevens, L. A.; Drage, T. C.; Snape, C. E.; Smith, M. W.; Adams, D. J.; Cooper, A. I. Porous organic alloys. *J. Am. Chem. Soc.* **2012**, *134*, 10741–10744.
53 Law, R. V.; Sherrington, D. C.; Snape, C. E. Solid-state ^{13}C MAS NMR studies of hyper-cross-linked polystyrene resins. *Macromolecules* **1996**, *29*, 6284–6293.
54 Liu, F.; Liang, W. D.; Wang, C. J.; He, J. X.; Xiao, C. H.; Zhu, Z. Q.; Sun, H. X.; Li, A. Superwetting monolithic hypercrosslinked polymers nanotubes with high salt-resistance for efficient solar steam generation. *Sol. Energy Mater Sol. Cells* **2021**, *221*, 110913.
55 Yan, Q.; Bai, Y. W.; Meng, Z.; Yang, W. T. Precipitation polymerization in acetic acid: synthesis of monodisperse cross-linked poly(divinylbenzene) microspheres. *J. Phys. Chem. B* **2008**, *112*, 6914–6922.
56 Li, H. Y.; Meng, B.; Mahurin, S. M.; Chai, S. H.; Nelson, K. M.; Baker, D. C.; Liu, H. L.; Dai, S. Carbohydrate based hyper-crosslinked organic polymers with -OH functional groups for CO_2 separation. *J. Mater. Chem. A* **2015**, *3*, 20913–20918.
57 Robshaw, T. J.; Jamesa, A. M.; Hammonda, D. B.; Reynolds, J.; Dawsona, R.; Ogden, M. D. Calcium-loaded hydrophilic hypercrosslinked polymers for extremely high defluoridation capacity *via* multiple uptake mechanisms. *J. Mater. Chem. A* **2020**, *8*, 7130–7144.
58 Wu, Y.; Li, L. G.; Yang, W. Y.; Feng, S. Y.; Liu, H. Z. Hybrid nanoporous polystyrene derived from cubic octavinylsilsesquioxane and commercial polystyrene *via* the Friedel-Crafts reaction. *RSC Adv.* **2015**, *5*, 12987–12993.
59 Yang, Z. Z.; Fu, S. Q.; Yan, C.; Yao, J. S.; Liu, W. L. Hyper-cross-linked polymers based on triphenylsilane for hydrogen storage and water treatment. *J. Macromol. Sci. A* **2018**, *56*, 162–169.
60 Gao, H.; Ding, L.; Bai, H.; Liu, A. H.; Li, S. Z.; Li, L. Pitch-based hyper-cross-linked polymers with high performance for gas adsorption. *J. Mater. Chem. A* **2016**, *4*, 16490–16498.

https://doi.org/10.1007/s10118-022-2667-7